ELSEVIER

Journal of Nuclear Materials 248 (1997) 140–146

journal of nuclear materials

Section 7. Tritium recovery from liquid breeders

Thermodynamics of the interactions between liquid breeders and ceramic coating materials

Peter Hubberstey *, Tony Sample [1]

Chemistry Department, Nottingham University, Nottingham NG7 2RD, United Kingdom

Abstract

The thermodynamic stabilities ($\Delta_r G$) of various ceramics towards Pb–Li alloys have been evaluated as a function of temperature, lithium composition and, for lithium, non-metal solute concentration. For non-metal saturated alloys, both increasing temperature and decreasing lithium composition (from lithium to Pb–17Li) lead to increased stability (more positive $\Delta_r G$ values). Reducing non-metal solute concentration in lithium by cold trapping leads to decreased stability. Of the ceramics presently being assessed as coating materials, AlN, TiN, TiC, Y_2O_3 and CaO are stable in reactor grade Pb–17Li and reactor grade lithium, β-SiC, Al_2O_3, SiO_2 and MgO are stable in Pb–17Li but not lithium and Cr_2O_3 is unstable in both breeders. © 1997 Elsevier Science B.V.

1. Introduction

Ceramic coatings for tritium breeder blanket containment materials are being developed to address the critical issues of magnetohydrodynamic pressure drops, high temperature corrosion and tritium loss [1]. Oxides (Al_2O_3, Cr_2O_3, Y_2O_3, SiO_2, CaO and MgO), nitrides (AlN, TiN) and carbides (β-SiC, TiC) are being assessed as potential barriers [2–4]. The possible deterioration of these coatings resulting in breakdown, spallation and impurity ingress into the liquid breeder blanket, is of fundamental importance to their development. Several groups [5–9] have studied the compatibility of oxides towards liquid Pb–17Li. Although most were found to be stable under proposed operating conditions (723–873 K) [6–8], SiO_2–Cr_2O_3 chemically densified coatings degraded significantly [5], owing to the reduction of Cr_2O_3. Under more extreme conditions (1073 K), $LiAl_5O_8$ and $LiAlO_2$ formation has also been observed on Al_2O_3 samples [9]. The compatibility of nitrides and carbides with Pb–17Li has been little studied; TiN, ZrC and β-SiC were recovered unchanged after exposure at 1073 K for 1500 h [9].

The majority of oxides has long been known [10,11] to be unstable towards lithium owing to the stability of Li_2O ($\Delta_f G^0(Li_2O, c, 773\ K) = -497.3$ kJ mol^{-1} [12,13]). Recently, one of those previously thought to be stable (Y_2O_3) has been shown to form $LiYO_2$ after contact with lithium at 773 K for 150 h [14], questioning the stability of all oxides. The use of nitrides and carbides in lithium is a more attractive option owing to the relative instability of Li_3N ($\Delta_f G^0(Li_3N, c, 773\ K) = -56.2$ kJ mol^{-1} [12,13]) and Li_2C_2 ($\Delta_f G^0(Li_2O, c, 773\ K) = -88.0$ kJ mol^{-1} [12,13]). However, early compatibility studies showed BN and Si_3N_4 to be unstable, forming Li_3BN_2 and Li_2SiN_2 [11].

In this paper, we report the results of thermodynamic calculations of the chemical stability of barriers in liquid Pb–Li alloys as a function of composition (x_{Li}, concentrating on Pb–17Li and lithium), non-metal solute concentration (x_X) and temperature, an integral part of which was the derivation of the thermodynamics of the Pb–Li system (specifically, $\overline{G}_{Li}$) as a function of x_{Li} and temperature.

2. Pb–Li thermodynamics

Following a recent critical analysis [15] of published thermodynamic data for the Pb–Li system we chose to derive lithium activities (a_{Li}) from emf data reported by

* Corresponding author. Tel.: +44-115 951 3509; fax: +44-115 951 3563; e-mail: peter.hubberstey@nottingham.ac.uk.

[1] Present address: BNFL, Research and Development, Sellafield, Seascale, Cumbria CA20 1PG, UK.

PII S0022-3115(97)00204-3

Table 1
Activity–temperature ($1.0 > x_{Li} > 0.1$) relationships for Pb–Li alloys. $\ln a_{Li} = A + B(T/K)^{-1}$

x_{Li}	A	B	Temperature range [a] (K)
0.1	−0.522	−7071	573–1023
0.2	−0.151	−6624	523–1023
0.3	0.415	−6378	613–1023
0.4	1.058	−6209	698–1023
0.5	1.652	−5996	755–1023
0.6	2.109	−5618	743–1023
0.7	2.284	−4951	915–1023
0.8	2.068	−3874	983–1023
0.9	1.346	−2264	823–1023

[a] Restricted by the formation of Li–Pb intermetallics, Li_8Pb_3 (m.p. 915 K), Li_3Pb (931 K), Li_7Pb_2 (999 K), $Li_{22}Pb_5$ (923 K).

Saboungi et al. [16] at 770, 812, 869 and 932 K. The data at 770 and 869 K are shown in Fig. 1 in the form of $\ln a_{Li}$ vs. x_{Li} isotherms. The plots fall into two sections with a marked change at $x_{Li} \sim 0.10$. We have considered the lead-rich data in a previous communication [15]. We now use the lithium-rich data to calculate firstly activity–temperature isocompositionals ($0.10 < x_{Li} < 1.00$) in the form

$$\ln a_{Li} = A + B(T/K)^{-1} \quad (1)$$

and secondly activity–composition isotherms ($523 < T(K) < 1023$) in the form

$$\ln a_{Li} = C + Dx_{Li} + Ex_{Li}^2 + Fx_{Li}^3, \quad (2)$$

where $A - F$ are constants.

Activity–temperature relationships are summarised in Table 1. Activity–composition isotherms ($773 < T(K) < 1023$) are shown in Fig. 1, which also includes a schematic representation of the pertinent section of the Li–Pb phase diagram [17]. The latter is included to indicate the limitations imposed on the use of these equations by the formation of high-melting intermetallics, Li_8Pb_3 (m.p. 915 K), Li_3Pb (931 K), Li_7Pb_2 (999 K) and $Li_{22}Pb_5$ (922 K) [17]. The agreement between the experimental activity data at 770 and 869 K and the calculated 773 and 873 K isotherms, clearly shown in Fig. 1, validates the mathematical analysis. The validity of these data was also checked by comparison of the derived $\bar{G}_{Li}$ ($= RT \ln a_{Li}$) values for Pb–17Li

$$\bar{G}_{Li} = -60.122 + 1778.2(T/K)^{-1} \quad (3)$$

with those reported earlier by Smith et al. [18]; in the temperature range 713–1013 K the difference is within 2 kJ mol^{-1}.

3. Thermodynamics of the interactions of Pb–Li alloys with ceramic coating materials

To assess the chemical viability of ceramic materials in liquid Pb–Li alloys, given by the free energy changes ($\Delta_r G$) of reactions of the type

$$M_xO_y(c) \xrightarrow{\text{liquid Pb–Li alloy}} yO(\text{Pb–Li}) + xM(c), \quad (4)$$

$$\Delta_r G = (1/x)\left\{y\bar{G}_O(\text{Pb–Li}) - \Delta_f G^0(M_xO_y)\right\} \quad (5)$$

(the reduced metal is assumed to be at unit activity) standard free energy of formation data for the ceramic ($\Delta_f G^0(M_xO_y, c, T)$) and solute free energy data in Pb–Li alloys ($\bar{G}_O$(Pb–Li)) are required. The former are available

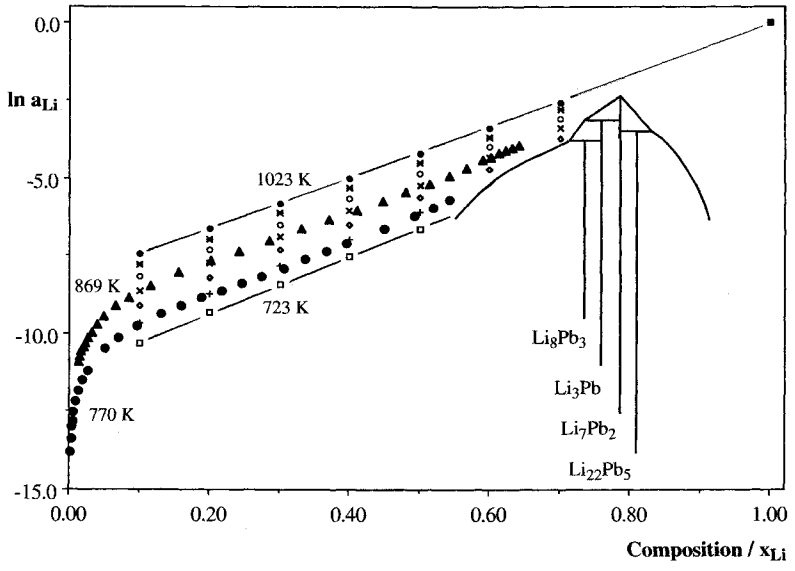

Fig. 1. Activity–composition relationships for Pb–Li alloys at 773 K. Calculated isotherms ($723 < T/K < 1023$) are compared with experimental data at 770 and 869 K. A schematic representation of the Pb–Li phase diagram is imposed to show the limitations imposed on the use of the isotherms by the formation of high melting Li_xPb_y intermetallics.

in critically assessed NBS compilations [12,13], the latter are given by expressions typified by

$$\overline{G}_O(\text{Pb–Li}) = RT \ln a_O = RT \ln a_O^* + RT \ln x_O/x_O^* = \Delta_f G^0(Li_2O) - 2\overline{G}_{Li}(\text{Pb–Li}) + RT \ln x_O/x_O^*, \quad (6)$$

where a_O^* is the oxygen activity at saturation, x_O is the oxygen composition and x_O^* is the oxygen composition at saturation [15]. Hence,

$$\Delta_r G = (1/x)\{y[\Delta_f G^0(Li_2O) - 2\overline{G}_{Li}(\text{Pb–Li}) + RT \ln x_O/x_O^*] - \Delta_f G^0(M_xO_y)\}. \quad (7)$$

To complete the calculations, solubility data for non-metals are required. The question of non-metal solubility in Pb–Li alloys is complex. Although all four lithium salts of the principal non-metal solutes (Li_2O, Li_3N, Li_2C_2 and LiH) can be formed from standard state non-metals in lithium, only Li_2O is sufficiently stable to be formed in Pb–17Li [15]. Hence free energy data can be derived for lithium systems using Eq. (7) and well established solubility expressions for oxygen, nitrogen and carbon in liquid lithium [19]:

$$\ln x_O = 1.428 - 6659(T/K)^{-1}, \quad 530 < T/K < 715,$$

$$\ln x_N = 2.976 - 4832(T/K)^{-1}, \quad 468 < T/K < 723,$$

$$\ln x_C = -1.100 - 5750(T/K)^{-1}, \quad 477 < T/K < 908.$$

For Pb–17Li systems, however, Eq. (7) is only strictly applicable for oxides. The solubility of oxygen in Pb–17Li is extremely small [20]. It follows that ingress of adventitious oxygen will maintain saturated solutions regardless of purification. The stability of the coating is then given by the simplified expression

$$\Delta_r G = (1/x)\{y[\Delta_f G^0(Li_2O) - 2\overline{G}_{Li}(\text{Pb–Li})] - \Delta_f G^0(M_xO_y)\}. \quad (8)$$

Clearly, $\Delta_r G$ data thus calculated are maximum (endothermic) values as $\overline{G}_O$(Pb–Li) becomes more exothermic with

Table 2
Free energy of reaction between various binary and ternary oxide coating materials and Pb–17Li or liquid lithium at 773 K (per g mol of metal)

Oxide	$\Delta_f G^\circ_{oxide}$ (kJ mol^{-1})	$\Delta_r G$ [a] (kJ mol metal^{-1})			Stability limit [b]
		O satd. Pb–17Li	O satd. lithium	473 K CT lithium	
Al_2O_3	−1432.6	143.8	−29.7	−82.3	[0.90]
Cr_2O_3	−927.7	−108.7	−282.2	−334.8	unstable
Fe_2O_3	−617.4	−263.8	−437.3	−490.0	unstable
Sc_2O_3	−1679.0	267.0	93.5	40.9	stable
Y_2O_3	−1678.8	266.8	93.4	40.7	stable
La_2O_3	−1570.4	212.7	39.2	−13.4	1.29×10^{-5}
Ce_2O_3	−1568.4	211.7	38.2	−14.5	1.42×10^{-5}
B_2O_3	−1072.5	−36.3	−209.8	−262.4	unstable
SiO_2	−770.3	6.9	−224.4	−294.6	0.20
TiO_2	−802.5	39.1	−192.1	−262.4	0.34
ZrO_2	−952.3	188.9	−42.3	−112.5	[0.90]
HfO_2	−974.0	210.6	−20.6	−90.9	0.95
CeO_2	−924.9	161.5	−69.7	−139.9	[0.82]
NiO	−168.9	−212.8	−328.4	−363.5	unstable
BeO	−533.0	151.3	35.7	0.6	stable
MgO	−517.4	135.7	20.1	−15.0	3.31×10^{-5}
CaO	−554.1	172.4	56.8	21.7	stable
$LiAlO_2$	−1024.4	203.2	29.7	−40.5	7.44×10^{-5}
$LiCrO_2$	−809.2	−12.0	−185.4	−255.7	unstable
$Li_2Si_2O_5$	−2183.5	79.7	−151.5	−239.3	0.52
Li_2SiO_3	−1408.4	147.7	−83.6	−188.9	[0.77]
Li_4SiO_4	−1963.1	205.1	−26.1	−166.6	0.93
Li_8SiO_6	−2963.9	211.2	−20.1	−230.7	0.95

[a] $\overline{G}_{Li} = RT \ln a_{Li}$ (= −57.8 kJ mol^{-1} for Pb–17Li; 0.0 kJ mol^{-1} for Li); $\overline{G}_O = RT \ln a_O^* - RT \ln x_O/x_O^*$ ($RT \ln a_O^* = \Delta_f G(Li_2O) - 2RT \ln a_{Li}$ (= −381.7 kJ mol^{-1} for Pb–17Li; −497.3 kJ mol^{-1} for Li); in lithium, $x_O = 3.21 \times 10^{-6}$ (at 473 K), $x_O^* = 7.57 \times 10^{-4}$ (at 773 K)).

[b] Quoted as either the lithium concentration (x_{Li}/mol fraction) above which, or the oxygen concentration (x_O/mol fraction) below which, barrier breakdown will occur. Compositions given in parentheses lie in the region bounded by the two phase sections (liquid + Li_8Pb_3) and (liquid + $Li_{22}Pb_5$).

increasing dilution (Eq. (6)). If required, the effect of dilution can be estimated from the corresponding data for liquid lithium systems. We have also considered the stabilities of nitrides and carbides in Pb–Li alloys using analogous expressions to Eq. (8). For lead-rich alloys including Pb–17Li, however, these equations are not applicable as the calculations assume that Li_3N and Li_2C_2 are stable in these liquids. Under these circumstances, the stability of the ceramics is effectively given by their standard free energy of formation.

Since ternary oxide formation has been observed by several authors [14,21,22] and has been shown to be thermodynamically favourable [15], the free energy changes ($\Delta_r G$) of reactions of the type

$$\mathrm{Li}_w\mathrm{M}_x\mathrm{O}_{y+z}(\mathrm{c}) \overset{\text{liquid Pb–Li alloy}}{\rightarrow} (y+z)\mathrm{O(Pb–Li)} + w\mathrm{Li(Pb–Li)} + x\mathrm{M(c)}, \quad (9)$$

$$\Delta_r G = (1/x)\left\{(y+z)\overline{G}_{\mathrm{O}}(\mathrm{Pb–Li}) + w\overline{G}_{\mathrm{Li}}(\mathrm{Pb–Li}) - \Delta_f G^0(\mathrm{Li}_w\mathrm{M}_x\mathrm{O}_{y+z})\right\}, \quad (10)$$

$$= (1/x)\left\{(y+z)\Delta_f G^0(\mathrm{Li_2O}) - (2y+2z-w)\overline{G}_{\mathrm{Li}}(\mathrm{Pb–Li}) + (y+z)RT\ln x_{\mathrm{O}}/x_{\mathrm{O}}^* - \Delta_f G^0(\mathrm{Li}_w\mathrm{M}_x\mathrm{O}_{y+z})\right\} \quad (11)$$

have also been calculated.

The results are collected in Table 2 (oxides) and Table 3 (nitrides and carbides); selected data are depicted in Figs. 2 and 3. They are directly comparable as they are given per mole of metal. The variation of $\Delta_r G$ with x_{Li} at 773 K is shown in Fig. 2 for selected oxides. Data are presented for oxygen saturated alloys in the composition range $0.1 < x_{\mathrm{Li}} < 0.7$, as well as for oxygen saturated lithium and lithium cold trapped at 473 K (i.e., lithium containing $x_{\mathrm{O}} = 3.207 \times 10^{-6}$ [19]). As noted earlier, the composition ranges are limited by the region of Li–Pb intermetallic formation (Fig. 1). In Fig. 2, the $\Delta_r G$ variation in this region is shown schematically by dashed lines. The stability of the ceramic decreases with increasing lithium content of the alloy (Fig. 2). Reducing the oxygen content of lithium results in reduced thermodynamic activities for the solute and hence more negative $\Delta_r G$ values.

The variation of $\Delta_r G$ with temperature is shown in Fig. 3 for the degradation of MgO (a typical example) in oxygen saturated Pb–17Li and lithium and in lithium containing different amounts of oxygen ($x_{\mathrm{O}} = 3.207 \times 10^{-6}$, 1.232×10^{-5} and 3.742×10^{-5}), as controlled by different cold trap temperatures (473, 523 and 573 K). For oxygen saturated solutions, increasing temperature results in more positive $\Delta_r G$ values. For unsaturated solutions, however, increasing temperature results in more negative $\Delta_r G$ values. As temperature is increased, the solubility of oxygen in liquid lithium increases leading, for a given oxygen content, maintained by a constant cold trap temperature, to greater $RT\ln x_{\mathrm{O}}/x_{\mathrm{O}}^*$ values (Eq. (6)) and hence to reduced oxygen thermodynamic activities. Fig. 3 also

Table 3
Free energy of reaction between various binary nitrides or carbides and liquid lithium at 773 K (per g mol of metal)

Ceramic	$\Delta_f G^{\circ}_{\mathrm{ceramic}}$ (kJ mol^{-1})	$\Delta_r G$ [a] (kJ mol metal^{-1})		Stability limit [b]
		satd. lithium	473 K CT lithium	
BN	−206.1	149.9	124.4	stable
AlN	−219.2	163.1	137.6	stable
Si_3N_4	−489.0	88.2	−13.8	1.11×10^{-3}
TiN	−263.7	207.6	182.1	stable
ZrN	−291.6	235.5	210.0	stable
VN	−150.2	94.1	68.6	stable
TaN	−187.6	131.5	106.0	stable
CrN	−61.6	5.5	−20.0	1.45×10^{-2}
β-SiC	−73.0	29.0	−1.3	2.13×10^{-6}
TiC	−175.0	131.0	100.7	stable
ZrC	−189.4	145.4	115.1	stable
NbC	−134.6	90.6	60.3	stable
TaC	−141.3	97.3	67.0	stable

[a] $\overline{G}_{\mathrm{N}} = RT\ln a_{\mathrm{N}}^* - RT\ln x_{\mathrm{N}}/x_{\mathrm{N}}^*$ ($RT\ln a_{\mathrm{N}}^* = \Delta_f G(\mathrm{Li_3N}) - 3RT\ln a_{\mathrm{Li}}$ (= −56.2 kJ mol^{-1} for Li); in lithium, $x_{\mathrm{N}} = 7.17\times10^{-4}$ (at 473 K), $x_{\mathrm{N}}^* = 0.0378$ (at 773 K)); $\overline{G}_{\mathrm{C}} = RT\ln a_{\mathrm{C}}^* - RT\ln x_{\mathrm{C}}/x_{\mathrm{C}}^*$ ($RT\ln a_{\mathrm{C}}^* = 0.5\Delta_f G(\mathrm{Li_2C_2}) - RT\ln a_{\mathrm{Li}}$ (= −44.0 kJ mol^{-1} for Li); in lithium, $x_{\mathrm{C}} = 1.75\times10^{-6}$ (at 473 K), $x_{\mathrm{C}}^* = 1.95\times10^{-4}$ (at 773 K)).

[b] Quoted as the nitrogen (or carbon) concentration (x_{X}/mol fraction) below which barrier breakdown will occur.

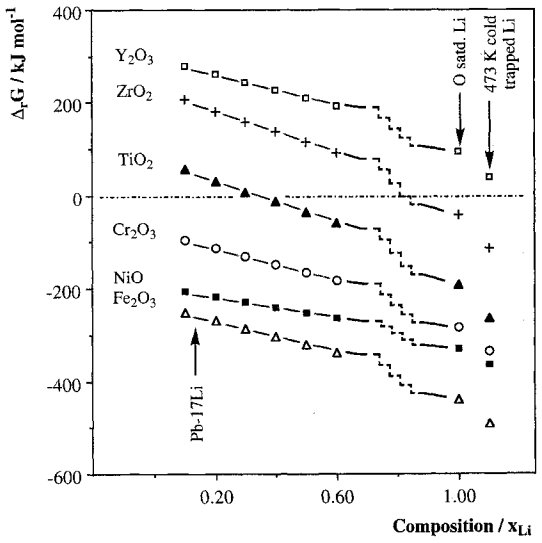

Fig. 2. Composition (x_{Li}) dependence of free energy data for the reaction of selected oxide ceramics with oxygen saturated Pb–Li alloys at 773 K. Data for 473 K cold trapped lithium ($x_{\mathrm{O}} = 3.21 \times 10^{-6}$) are also included.

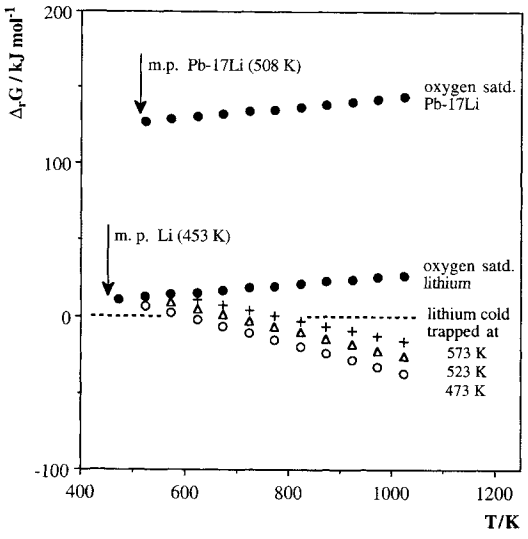

Fig. 3. Temperature dependence of free energy data for the reaction of MgO with oxide saturated Pb–17Li and with lithium (both oxide saturated and cold trapped at 473 ($x_O = 3.21 \times 10^{-6}$), 523 ($1.23 \times 10^{-5}$) or 573 K ($3.74 \times 10^{-5}$)).

shows that ceramics are much more stable in Pb–17Li than in lithium and that reducing the non-metal content of lithium by cold trapping destabilises the ceramic.

The stability of tritium permeation barriers in liquid Pb–17Li has been discussed previously [2]. Inspection of Tables 2 and 3 reveals that whereas all the binary carbides and nitrides are stable, the binary oxides display a diversity of behaviour. Although the majority are stable, Cr_2O_3, Fe_2O_3, B_2O_3 and NiO reduce to the metal and SiO_2 has a $\Delta_r G$ value close to zero. The fact that the nitrides and carbides are more stable than the oxides is due, not to their intrinsic stabilities, but to the fact that Li_3N and Li_2C_2 are much less stable than Li_2O [19].

Ternary oxides are intrinsically more stable to reduction to the metal than their binary counterparts, their stabilities increasing with increasing Li_2O content, e.g., from $Li_2Si_2O_5$ through Li_2SiO_3 and Li_4SiO_4 to Li_8SiO_6 (Table 2). This observation is consistent with the fact that conversion of the binary oxides to the ternary oxides is favourable [2]. $LiCrO_2$ is the only ternary oxide that is predicted to be unstable; the calculated $\Delta_r G$ value, however, is close to zero (Table 2).

The situation is similar in liquid lithium, but there is a greater tendency to decomposition especially in 473 K cold trapped lithium. Although only CrN, Si_3N_4 and β-SiC of the nitrides and carbides are predicted to be unstable (Table 3), of the oxides (both ternary and binary) only four (Sc_2O_3, Y_2O_3, CaO and BeO) are predicted to be stable (Table 2) and of these BeO has a $\Delta_r G$ value close to zero (Table 2). Those oxides proposed as suitable coatings for use in Pb–17Li (Al_2O_3, Cr_2O_3, SiO_2 and MgO) are not applicable in liquid lithium. The ternary oxides are more stable than the corresponding binary oxides. Hence, since binary to ternary oxide conversion is favourable, Y_2O_3 and Sc_2O_3, despite being thermodynamically stable to reduction, may undergo conversion to $LiYO_2$ and $LiScO_2$ as noted by Terai [14].

This analysis assumes that the reduced metals are generated at unit activity. Although this is a realistic assumption for the majority, aluminium and silicon are highly soluble in liquid lithium and so will have markedly reduced activities. Thus, aluminium and silicon containing ceramics will be destabilised relative to the data in Tables 2 and 3.

4. Thermodynamics of the self-healing of ceramic coatings

The question of the self-healing properties of chemically stable coatings now arises. Clearly, only those coatings which may be fabricated by surface oxidation methods (as opposed to plasma spraying, chemical vapour deposition, chemically densified coating or ion implantation methods) may undergo self-healing processes; these include Al_2O_3 coatings produced by oxidation of aluminium deposited on steel surfaces and Cr_2O_3 coatings produced by oxidation of steel surfaces.

Annealing of aluminium deposited on steel surfaces leads to an aluminium concentration gradient throughout the coating with Al-rich species (θ-$FeAl_3$, η-Fe_2Al_5 and ζ-$FeAl_2$) at the surface and Fe-rich species (β′-FeAl, β″-Fe_3Al and α-Fe (a solid solution of Al in Fe ($0.0 < x_{Al} < 0.2$))) adjacent the base steel [2]. We have recently analyzed the thermodynamics of the Fe–Al system to generate $\overline{G}_{Al}$ values as a function of temperature and x_{Al} [2]. The preceding discussion indicates that unit activity aluminium should react with oxygen-saturated Pb–17Li, but not lithium, to form either Al_2O_3 or $LiAlO_2$. Reduction of a_{Al} will result in less negative $\Delta_r G$ values, eventually leading, at a sufficiently low a_{Al} values, to no reaction. Consequently, self healing is critically dependent on a_{Al}. To determine the conditions for self healing, we have calculated $\Delta_r G$ values for the reactions

$$2Al(Fe\text{–}Al\ alloy) + 3O(Pb\text{–}Li) \rightarrow Al_2O_3(c), \quad (12)$$

$$\Delta_r G = (1/2)\{\Delta_f G^0(Al_2O_3) - \{2\overline{G}_{Al}(Fe\text{–}Al) + 3\overline{G}_O(Pb\text{–}Li)\}\}, \quad (13)$$

$$= (1/2)\{\Delta_f G^0(Al_2O_3) - \{2\overline{G}_{Al}(Fe\text{–}Al) + 3\Delta_f G^0(Li_2O) - 6\overline{G}_{Li}(Pb\text{–}Li) + 3RT \ln x_O/x_O^*\}\}, \quad (14)$$

$$Al(Fe\text{–}Al\ alloy) + Li(Pb\text{–}Li) + 2O(Pb\text{–}Li) \rightarrow LiAlO_2(c), \quad (15)$$

$$\Delta_r G = \Delta_f G^0(LiAlO_2) - \{\overline{G}_{Al}(Fe\text{–}Al) + \overline{G}_{Li}(Pb\text{–}Li) + 2\overline{G}_O(Pb\text{–}Li)\}, \quad (16)$$

$$= \Delta_f G^0(LiAlO_2) - \{\overline{G}_{Al}(Fe\text{–}Al) - 3\overline{G}_{Li}(Pb\text{–}Li) + 2\Delta_f G^0(Li_2O) + 2RT \ln x_O/x_O^*\} \quad (17)$$

as a function of x_{Al}, x_{Li}, x_O and temperature.

The results for $LiAlO_2$ formation at 773 K are summarised in Table 4; $\Delta_r G$ values are given for reactions of Fe–Al alloys with Pb–17Li (oxygen saturated) and with lithium (oxygen saturated and 473 K cold trapped). $\Delta_r G$ values for Al_2O_3 formation are less exothermic by 59.41 kJ mol^{-1} (oxygen saturated Pb–Li alloys) or 41.85 kJ mol^{-1} (473 K cold trapped lithium). Also included in Table 4 are either the maximum lithium concentration required for reaction (assuming oxygen saturated Pb–Li alloy) or the minimum oxygen concentration required for reaction in lithium.

The calculations predict that self-healing of aluminide coatings will occur in oxygen saturated Pb–17Li, regardless of x_{Al}. In an earlier detailed analysis of self-healing of aluminide coatings in Pb–17Li [2] we concluded that the minimum x_{Al} required for Al_2O_3 and $LiAlO_2$ formation are $x_{Al} = 0.0133$ and 0.0015 in oxygen saturated Pb–17Li at 773 K. In 473 K cold trapped lithium, however, self-healing will not occur; a_O is too low. For conversion of pure aluminium and ζ-Al_3Fe into $LiAlO_2$, the minimum oxygen content required is $x_O = 0.748 \times 10^{-4}$ and 5.660×10^{-4}, respectively. For alloys of lower aluminium content, self healing will only occur in Pb–Li alloys (Table 4).

Although the stability calculations suggest that both $LiCrO_2$ and Cr_2O_3 are unstable in both Pb–17Li and lithium, the fact that there are several literature reports of $LiCrO_2$ formation on oxidised steel surfaces in Pb–17Li [21,22] prompted us to consider, as a function of both x_{Li} and temperature, the formation of $LiCrO_2$ and Cr_2O_3. Substrates considered were chromium metal, 316 stainless steel and Cr_7C_3, one of the chromium carbides ($Cr_{23}C_6$, Cr_7C_3 and Cr_3C) thought to be formed in the grain boundaries of steels [23]. Similar expressions to Eqs. (14) and (17) were used. $\overline{G}_{Cr}$ data for the steel were derived from a_{Cr} data reported by Gnanamoorthy et al. for AISI 316LN steel ($\log a_{Cr} = -0.13 + 54.95(T/K)^{-1}$ [24]). The calculated $\Delta_r G$ values for oxygen saturated Pb–17Li, depicted in Fig. 4, are endothermic throughout; those for lithium are even more endothermic (+173.44 kJ mol^{-1} at 773 K for oxygen satd. lithium). The $\Delta_r G$ values for formation of $LiCrO_2$ on 316 SS immersed in oxygen saturated Pb–17Li (= 20.00 kJ mol^{-1} at 773 K (Fig. 4)) is particularly sensitive to the calculated $\overline{G}_{Li}$ data; an error of 6.7 kJ mol^{-1} would be sufficient to give an incorrect prediction. They also rely on uncorroborated $\Delta_f G^0(LiCrO_2)$ data obtained from electrochemical measurements of $Cr/Cr_2O_3/LiCrO_2//CaF_2$–$LiF//Co/CoF_2$ cells [25]. All the other standard free energy of formation data are taken from critically assessed NBS compilations [19].

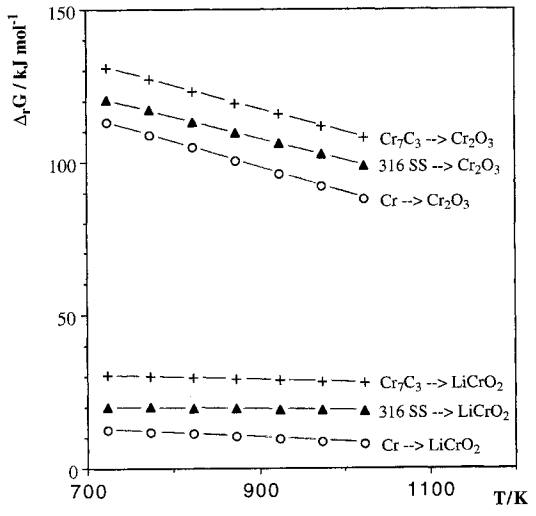

Fig. 4. Temperature dependence of free energy data for the reaction of chromium, AISI 316LN SS and Cr_7C_3 with oxide saturated Pb–17Li to form Cr_2O_3 and $LiCrO_2$.

Table 4
Free energy (kJ mol^{-1}) of reaction between Fe–Al alloys and Pb–17Li (oxygen saturated) or lithium (oxygen saturated or 473 K cold trapped) at 773 K (per g mol of metal)

Fe–Al alloy	Pb–17Li (O satd.)	Lithium		x_{Li} [a]	$10^4 x_O$ [b]
		(O satd.)	473 CT		
Pure Al	−203.2	−29.8	40.5	–	0.75
θ-$FeAl_3$	−182.8	−9.4	60.9	–	3.65
η-Fe_2Al_5	−177.2	−3.7	66.5	–	5.66
ζ-$FeAl_2$	−176.6	−3.1	67.1	–	5.95
β ($x_{Al} = 0.5$)	−158.5	14.9	85.1	0.95	–
α ($x_{Al} = 0.2$)	−133.5	39.9	110.2	0.86	–
α ($x_{Al} = 0.1$)	−114.6	58.9	129.1	0.79	–
α ($x_{Al} = 0.01$)	−51.7	121.8	192.0	0.48	–

[a] Maximum lithium concentration for reaction (assuming oxygen saturated Pb–Li alloy).
[b] Minimum oxygen concentration required in lithium for reaction ($x_O = 7.567 \times 10^{-4}$ at saturation at 773 K [19]).

5. Conclusions

Temperature, lithium content and non-metal solute concentration affect the stabilities of ceramics ($\Delta_r G$) in breeder materials. Increasing temperature and decreasing lithium content lead to more positive $\Delta_r G$ values (increased stability), but reducing the solute concentration in lithium by cold trapping leads to more negative $\Delta_r G$ values (decreased stability).

The thermodynamic predictions are generally in agreement with experimental observations [5–11]. In oxide saturated liquid Pb–17Li the majority of binary oxides (e.g., MgO, Al_2O_3) are stable with respect to reduction to the metal; only a limited number (e.g., SiO_2, Cr_2O_3) are unstable. The corresponding ternary oxides (e.g., $LiAlO_2$, Li_2SiO_3, $LiCrO_2$) are intrinsically more stable to reduction to the metal, only $LiCrO_2$ being unstable. The binary carbides (e.g., β-SiC) and nitrides (e.g., TiN) considered are stable.

In reactor grade lithium (cold trapped at 473 K), all the binary oxides (except Y_2O_3, Sc_2O_3 and CaO) and ternary oxides are unstable. On the other hand, the binary nitrides (except Si_3N_4 and CrN) and carbides (except β-SiC) are stable.

The predicted instability of Cr_2O_3 and $LiCrO_2$ supports the degradation of Cr_2O_3 containing barriers noted in liquid Pb–17Li [5] but conflicts with the $LiCrO_2$ formation observed on steels in liquid Pb–17Li [21,22].

Since conversion of the binary oxides to the ternary oxides is invariably favourable in oxide saturated systems, in agreement with the observed conversion of Y_2O_3 into $LiYO_2$ in lithium [14] and of Al_2O_3 into $LiAlO_2$ and $LiAl_5O_8$ in Pb–17Li [9], the predicted stability of the nitrides and carbides should be considered with caution owing to the possible formation of ternaries for which reliable free energy data are not available.

Aluminide barriers are predicted to self-heal in Pb–17Li but not in lithium cold trapped at 473 K. In oxide saturated Pb–17Li at 773 K, formation of Al_2O_3 and $LiAlO_2$ (the thermodynamically favoured product) is predicted for Fe–Al alloys with $x_{Al} \geq 0.0133$ and 0.0015, respectively. In lithium at 773 K, only high activity aluminium sources are predicted to react to form $LiAlO_2$, and only in the presence of high oxygen activities. The minimum oxygen content required for reaction with pure aluminium is $x_O = 0.748 \times 10^{-4}$, a highly improbable scenario.

References

[1] A. Perujo, K. Forcey, Fusion Eng. Des. 28 (1995) 252.
[2] P. Hubberstey, T. Sample, A. Terlain, Fusion Technol. 28 (1995) 1194.
[3] T. Tanabe, Fusion. Technol. 28 (1995) 1278.
[4] H. Glasbrenner, H.U. Borgstedt, Z. Peric, in: Liquid Metal Systems, ed. H.U. Borgstedt (Plenum, New York, 1995) p. 95.
[5] T. Terai, T. Yoneoka, H. Tanaka, H. Kawamura, M. Nakamichi, K. Miyajima, J. Nucl. Mater. 212–215 (1994) 976.
[6] A. Terlain, T. Flament, J. Sannier, J.L. Rouault, Fusion Technol. 2 (1991) 916.
[7] I. Schreinlechner, P. Sattler, J. Nucl. Mater. 191–194 (1992) 970.
[8] H.U. Borgstedt, H. Glasbrenner, Z. Peric, J. Nucl. Mater. 212–215 (1994) 1501.
[9] V. Coen, H. Kolbe, L. Orecchia, M. Della Rossa, High Temperature Corrosion of Technical Ceramics (Elsevier Applied Science, Amsterdam, 1989).
[10] R.N. Singh, J. Am. Ceram. Soc. 59 (1976) 112.
[11] I. Schreinlechner, F. Holub, in: Liquid Metal Systems, ed. H.U. Borgstedt (Plenum, New York, 1982) p. 105.
[12] M.W. Chase, C.A. Davis, J.R. Downey, D.J. Frurip, R.A. McDonald, A.N. Syverud, J. Phys. Chem. Ref. Data 14 (1) (1985).
[13] C.E. Wicks, F.E. Block, US Bureau of Mines Bulletin 606 (1963).
[14] T. Terai, European Workshop on Lithium and Pb–17Li Corrosion and Chemistry, Nottingham, 1995, personal communication.
[15] P. Hubberstey, T. Sample, J. Nucl. Mater. 199 (1993) 149.
[16] M.L. Saboungi, J. Marr, M. Blander, J. Chem. Phys. 68 (1978) 1375.
[17] A.D. Moffatt, Moffatt's Handbook of Binary Phase Diagrams (1992).
[18] D.L. Smith, G.D. Morgan, USDOE Report ANL/FPP-84-1, Vol. 2, 1984, p. 6-1.
[19] P. Hubberstey, A.T. Dadd, P.G. Roberts, in: Liquid Metal Systems, ed. H.U. Borgstedt (Plenum, New York, 1982) p. 445.
[20] M.G. Barker, J.A. Lees, T. Sample, in: Proc. 4th. Int. Conf. Liquid Metal Eng. and Technol., Avignon, Vol. 1, Paper 206, 1984.
[21] M.G. Barker, V. Coen, H. Kolbe, J.A. Lees, L. Orecchia, T. Sample, J. Nucl. Mater. 155–157 (1988) 732.
[22] T. Sample, V. Coen, H. Kolbe, L. Orecchia, J. Nucl. Mater. 191–194 (1992) 979.
[23] M. Hirai, A. Kozuru, M. Yamawaki, M. Kanno, J. Nucl. Sci. Technol. 20 (1983) 333.
[24] A.M. Azad, O.M. Sreedharan, J.B. Gnanamoorthy, J. Nucl. Mater. 167 (1989) 82.
[25] N.P. Bhat, K. Swaminathan, D. Krishnamurthy, O.M. Sreedharan, Liquid Metal Engineering and Technology, Vol. 1 (BNES, London, 1984) p. 323.